# Elastic electron scattering from formic acid

C. S. Trevisan,[1] A. E. Orel,[1] and T. N. Rescigno[2]

[1]*Department of Applied Science, University of California, Davis, CA 95616*
[2]*Chemical Sciences, Lawrence Berkeley National Laboratory, Berkeley, CA 94720*

(Dated: February 15, 2006)

Following our earlier study on the dynamics of low energy electron attachment to formic acid, we report the results of elastic low-energy electron collisions with formic acid. Momentum transfer and angular differential cross sections were obtained by performing fixed-nuclei calculations employing the complex Kohn variational method. We make a brief description of the technique used to account for the polar nature of this polyatomic target and compare our results with available experimental data.

PACS numbers: 34.80.Gs

## I. INTRODUCTION

Low-energy electron collisions initiate and drive much of the relevant chemistry associated with radiation damage in biomolecules. Although traditional thinking attributed radiation damage of biological molecules to high-energy primary ionizing radiation events, recent experiments of Leon Sanche and collaborators [1, 2] showed that it is the numerous low-energy secondary electrons produced by the primary ionizing radiation energy that play a key role in causing single and double strand breaks in crystal DNA, especially at energies well below ionization threshold.

Sanche's landmark findings have opened new fields of exploration regarding low-energy collisions with biomolecules, because it now appears that resonant collisions may be an important mechanism in radiation damage of biological systems. Formic acid (HCOOH), the simplest organic acid, is of interest to both biological and astronomical environments in that sense. It is of interest to the astronomy community because dense clumps of formic acid were found in hot interstellar molecular cores and because it is believed to be important in the formation of biological molecules such as acetic acid and glycine, which have also been observed in space. Glycine is the simplest amino acid. Amino acids are the building blocks of proteins and DNA. The connection between formic acid and more complex biologically important molecules makes the electron-formic acid system relevant not only to astronomy, but also to numerous biological applications.

There has been several experimental measurements of dissociative electron attachment to formic acid [3–6]. These measurements show that low-energy electron collisions with formic acid and other simple organic acids (for example glycine and alanine, among others) will result in the production of fragment negative ions by dissociative attachment. In the case of formic acid, the measured dissociative attachment reaction with lowest incident electron energy (of approximately 1.3 eV) is:

$$HCOOH + e^- \rightarrow (HCOOH^-) \rightarrow HCOO^- + H$$

In an investigation carrier out recently, we explored the mechanisms of low energy electron attachment to formic acid and identified a dissociation pathway to illustrate the importance of intrinsic polyatomic effects in the dissociation dynamics of this system. To the best of our knowledge, only one other calculation of low-energy electron scattering by gas phase formic acid has been performed by Gianturco and Lucchese [7]. They used a local potential model to perform calculations at the equilibrium geometry of both *trans* and *cis* formic acid. They found two resonances, one around 3.5 eV and the other one near 12 eV, which they interpreted as probable precursor states for the metastable anion $(HCOOH)^-$ that decays into the dissociation channels that have been observed experimentally.

In the present investigation, we report *ab initio* elastic differential and momentum transfer cross sections of low-energy electron scattering from formic acid obtained by employing the complex Kohn variational method. We performed fixed-nuclei calculations at the equilibrium geometry of *trans* formic acid. Formic acid possesses a permanent dipole moment. Angular differential cross sections obtained by fixed-nuclei calculations of electron scattering by a polar molecule will diverge in the forward direction and, hence, will produce infinite total cross sections. To obtain meaningful cross sections, we therefore utilized a treatment in which the higher order partial-wave components of the T-matrix are included in the Born approximation via a closure formula (see [8] and the references therein). Our results are compared with recent experimental measurements [9].

In the following section, we will make a brief description of the theoretical treatment we have used. Section III outlines the computational details of the present study. Our results, compared to available experimental measurements, are also presented in this section. We conclude with a brief summary.

## II. THEORY

### A. Complex Kohn variational method

The complex Kohn method is a variational technique which uses a trial wave function that is expanded in terms of square-integrable (Cartesian Gaussian) and continuum basis functions that incorporate the correct asymptotic boundary conditions. Detailed descriptions of the method have been given in previous publications [10, 11], so only a brief summary of the aspects that concern this study will be given below.

In the case of electronically elastic scattering, the trial wave function takes the form:

$$\Psi = \mathcal{A}[\Phi_o(\vec{r}_1..\vec{r}_N)F(\vec{r}_{N+1})] + \sum_\mu d_\mu \Theta_\mu(\vec{r}_1..\vec{r}_{N+1}) \quad (1)$$

where $\Phi_o$ is the wave function that describes the ground-state of the target molecule, $\mathcal{A}$ antisymmetrizes the coordinates of the incident electron ($\vec{r}_{N+1}$) with those of the target and the sum contains square-integrable, $(N+1)$ - electron terms that describe polarization and/or correlation effects due to electronically closed channels. In the present study, these configuration-state functions (CSFs), $\Theta_\mu$, were constructed by singly exciting the occupied orbitals. More details about the construction of these CSFs will be given in section III. The scattering function, $F(\vec{r}_{N+1})$, is further expanded in the Kohn method in a combined basis of Gaussian ($\phi_i$) and continuum (Ricatti-Bessel, $j_l$,and Hankel, $h_l^+$) basis functions

$$F(\vec{r}) = \sum_i c_i\phi_i(\vec{r}) + \sum_{lm}[j_l(kr)\delta_{ll_o}\delta_{mm_o} + T_{ll_omm_o}h_l^+(kr)]Y_{lm}(\hat{r})/r. \quad (2)$$

where $Y_{lm}(\hat{r})$ are spherical harmonics. Applying the stationary principle for the $T$-matrix,

$$T_{stat} = T_{trial} - 2\int \Psi(H-E)\Psi \quad (3)$$

results in a set of linear equations for the coefficients $c_i$, $d_\mu$ and $T_{ll_omm_o}$. The T-matrix elements, $T_{ll_omm_o}$, are the fundamental dynamical quantities from which all fixed-nuclei cross sections are derived.

### B. Polar molecule treatment

As mentioned in the introduction, fixed-nuclei calculations of electron scattering by molecules that possess a permanent dipole moment will produce infinite total cross sections and angular differential cross sections that diverge in the forward direction [12]. To tackle this added difficulty, we used the approach of Rescigno and Lengsfield, in which only the low order partial wave components of the T-matrix are obtained from variational calculations, whereas the higher order terms are included in the Born approximation via a closure formula. Details of this treatment can be found in [8]. Here, we will only outline the basic concepts behind this technique.

The adiabatic approximation usually employed in electron-molecule scattering allows for the rotational motion of the target molecule to be neglected during the collision. But the conditions that validate the adiabatic approximation are not satisfied in the case of polar molecules, due to the long-range nature of the electron-dipole interaction. Even though the adiabatic approximation cannot be used to obtain total cross sections in the case of electron scattering by polar molecules, it can be employed to describe scattering at angles other than zero, as well as momentum transfer cross sections.

In the fixed-nuclei approximation, cross sections are obtained from the T-matrix by averaging over all orientations of the target molecule. In the treatment employed in this study, the Born closure is applied to the T-matrix itself (rather than to the differential cross section). The fixed-nuclei T-matrix for a fixed point dipole can then be written as [12]

$$T = {}^BT + \sum_{\substack{ll'\\mm'}} i^{l-l'}Y^*_{l'm'}(\widehat{\mathbf{k}}')Y_{l'm'}(\widehat{\mathbf{k}})(T_{lml'm'} - {}^BT_{lml'm'}) \quad (4)$$

where the first and last terms are the full Born T-matrix for a fixed point dipole and its partial wave expansion, respectively. The partial-wave first Born T-matrix elements are defined in [8].

The sum in Eq.(4) will converge rapidly, because it involves differences between exact and first Born partial-wave T-matrix elements. The differential cross sections are obtained by numerical quadrature of the integrations in

$$\frac{d\sigma}{d\omega} = \frac{(4\pi)^2}{k^2}\int \frac{d\alpha d\cos\beta d\gamma}{8\pi^2}\left|\langle \mathbf{k}'|T^{\Gamma\Gamma'}|\mathbf{k}\rangle\right|^2 \quad (5)$$

where the integration is over the Euler angles that orient wave vectors $\mathbf{k}$ and $\mathbf{k}'$ with respect to the target. The angle between $\mathbf{k}$ and $\mathbf{k}'$ is the laboratory scattering angle.

## III. CALCULATIONS AND RESULTS

We performed fixed-nuclei scattering calculations using the complex Kohn method. The basis set used is the triple-zeta contraction of the [9s,5p,1d] oxygen and carbon Gaussian basis functions of Dunning [13] centered at each atom, augmented with an additional diffuse p-function ($\alpha = 0.059$) on the oxygens. For the hydrogens,

we used Dunning's [4s,1p] Gaussian basis set, again centered at each atom. The target molecular orbitals were obtained by performing a self-consistent field (SCF) calculation on the closed shell ground state of the equilibrium geometry of *trans* HCOOH. The equilibrium nuclear positions were optimized at the SCF level. Coordinates resulting from this optimization and used for the fixed-nuclei calculations are given in Table I. As can be seen by looking at this table, at its equilibrium geometry, formic acid is a planar molecule belonging to the point group $C_s$. With coordinates as described in Table I, its permanent dipole moment lies along the z-axis. We found the dipole moment of HCOOH to be ∼-0.678141 a.u.

TABLE I: Optimized geometry for the neutral ground state of *trans* formic acid. Coordinates are in atomic units, where $a_o = 5.2917721 \times 10^{-11}$ m is the Bohr radius.

| Atomic center | x($a_o$) | y($a_o$) | z($a_o$) |
|---|---|---|---|
| C | 0.000000 | 0.000000 | 0.000000 |
| O | 0.775100 | 0.000000 | 2.091570 |
| O | 1.428910 | 0.000000 | -2.050200 |
| H | -1.984090 | 0.000000 | -0.504453 |
| H | 3.154391 | 0.000000 | -1.558650 |

The short-range correlation and long-range polarization part of the complex Kohn trial function was constructed by including all CSFs generated by placing six electrons in the three frozen core orbitals (carbon and oxygen 1s) and by singly exciting the occupied target orbitals into all unoccupied virtual orbitals whose orbital energies were less than two hartrees. The expansion of the trial scattering function was completed by including numerically generated continuum basis functions, retaining terms with angular momentum quantum numbers $l$ and $|m|$ less than or equal to 5. In the calculation of momentum transfer and angular differential cross sections, terms with angular momentum quantum numbers $l$ and $|m|$ greater than 5 were accounted for by employing the Born correction, as described in the previous section.

Figures 1 through 3 show the momentum transfer and differential cross sections obtained from the first-Born corrected matrix. Whenever available, we compared our calculations with experimental measurements of Vizcaino *et al.* [9]. Vizcaino *et al.* studied elastic electron scattering from formic acid using a crossed-beam electron spectrometer. They measured absolute differential cross sections for the first time by employing the relative flow technique, where flow rates for HCOOH and a reference gas (He) are measured at a number of temperatures.

Fixed-nuclei elastic scattering calculations revealed a resonance at ∼1.9 eV with a width of ∼0.2 eV, depicted in figure 1, which illustrates the momentum transfer cross section of elastic electron scattering from HCOOH. Figure 2 shows our calculated angular differential cross sections at scattering electron energies close to that of the shape resonance, compared against the experimental data of Vizcaino *et al.* Circles with error bars represent

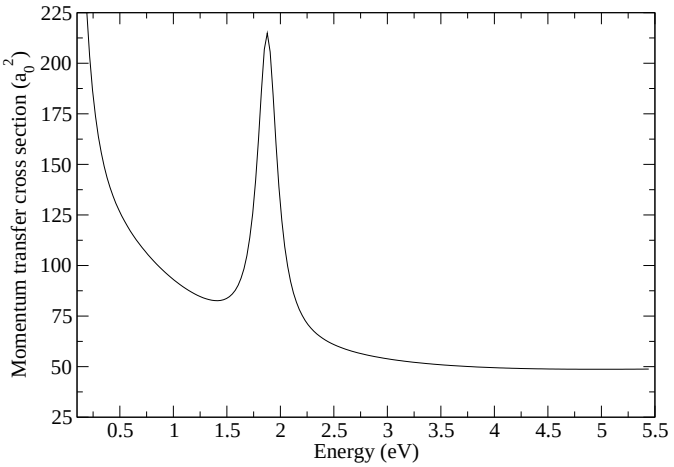


FIG. 1: Electron scattering from formic acid: momentum transfer cross sections. Cross sections are in atomic units ($a_o^2 = 2.8002852 \times 10^{-21}$ m$^2$). Energies are in units of eV = $1.6021765 \times 10^{-19}$ J.

the experimental measurements at an incident electron energy of 1.8 eV. All cross sections have been plotted on an absolute scale, with no inter-normalization. At an incident electron energy of 1.8 eV (dash-dot curve), our cross section has the same shape, but overestimates the magnitude of the experimental values. This discrepancy is expected for differential cross sections calculated at energies that lie in the vicinity of the resonance energy. As we move away from the resonance energy, the calculated differential cross sections will approach the experimental measurements in both shape and magnitude, as can be seen in figure 2 in the case of calculated cross sections at 1.6 eV (solid curve), 1.7 eV (dash curve) and 2.0 eV (double dash-dot curve).

Figure 3 shows angular differential cross sections at selected energies of the incident electron. At energies at which experimental measurements are available (5 and 10 eV), the agreement between calculated and measured cross sections is reasonably good.

## IV. SUMMARY

We have presented the results of a theoretical study of elastic electron scattering from formic acid at low incident electron energies (0.1-10 eV). We performed fixed-nuclei calculations employing the complex Kohn method and determined the low order partial-wave components of the T-matrix variationally. Due to the polar nature of formic acid, we included the high order partial wave components of the T-matrix in the Born approximation via a closure formula, which allowed us to extract meaningful momentum transfer and differential cross sections. We compared our results with available experimental measurements and obtained a reasonably good agreement.

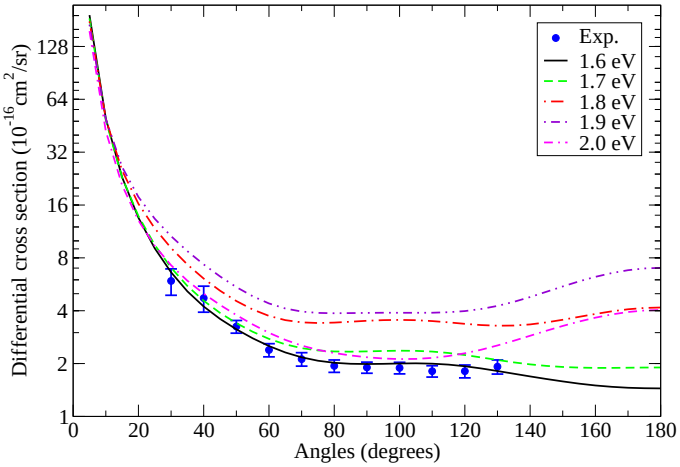


FIG. 2: (Color online) Electron scattering from formic acid: angular differential cross sections. Circles with error bars: experimental data of Vizcaino *et al.* [9] at an incident electron energy of 1.8 eV. Solid curve: complex Kohn calculations at 1.6 eV. Dash curve: complex Kohn calculations at 1.7 eV. Dash-dot curve: complex Kohn calculations at 1.8 eV. Dash-double dot curve: complex Kohn calculations at 1.9 eV. Double dash-dot curve: complex Kohn calculations at 2.0 eV. Differential cross sections are in units of $10^{-16}$ cm$^2$/sr and energies are in eV.

**Acknowledgments**

Work at the University of California Lawrence Berkeley National Laboratory was performed under the auspices of the US Department of Energy under contract DE-AC02-05CH11231 and was supported by the U.S. DOE Office of Basic Energy Sciences, Division of Chemical Sciences. A.E.O. also acknowledges support from the National Science Foundation (Grant No. PHY-02-44911).

[1] L. Sanche, Eur. Phys. J. D **35**, 367 (2005).
[2] Boudaïffa, P. Cloutier, D. Hunting, M. A. Huels, and L. Sanche, Science **287**, 1658 (2000).
[3] A. Pelc, W. Sailer, P. Scheier, N. J. Mason, E. Illenberger, and T. D. Märk, Vacuum **70**, 429 (2003).
[4] A. Pelc, W. Sailer, P. Scheier, N. J. Mason, and T. D. Märk, Eur. Phys. J. D **20**, 441 (2002).
[5] A. Pelc, W. Sailer, P. Scheier, M. Probst, N. J. Mason, E. Illenberger, and T. D. Märk, Chem. Phys. Lett. **361**, 277 (2002).
[6] K. Aflatooni, B. Hitt, G. A. Gallup, and P. D. Burrow, J. Chem. Phys. **115**, 6489 (2001).
[7] F. A. Gianturco and R. R. Lucchese, New J. Phys. **6**, 66 (2004).
[8] T. N. Rescigno and B. H. Lengsfield, Z. Phys. D **24**, 1992 (117-124).
[9] V. Vizcaino, M. Jelisavcic, J. P. Sullivan, and S. J. Buckman, *Private Communications and Program of the 58th Annual Gaseous Electronics Conference*, vol. 50, No.7 (American Physical Society, 2005).
[10] T. N. Rescigno, C. W. McCurdy, A. E. Orel, and B. H. Lengsfield, *Computational Methods for Electron-Molecule Collisions* (eds. W. M. Huo and F. A. Gianturco, Plenum, New York, 1995).
[11] T. N. Rescigno, B. H. Lengsfield, and C. W. McCurdy, *Modern Electronic Structure Theory*, vol. 1 (ed. D. R. Yarkony, World Scientific, Singapore, 1995).
[12] O. H. Crawford, A. Dalgarno, and P. B. Hays, Mol. Phys. **13**, 181 (1967).
[13] T. H. Dunning, J. Chem. Phys. **53**, 2823 (1970).

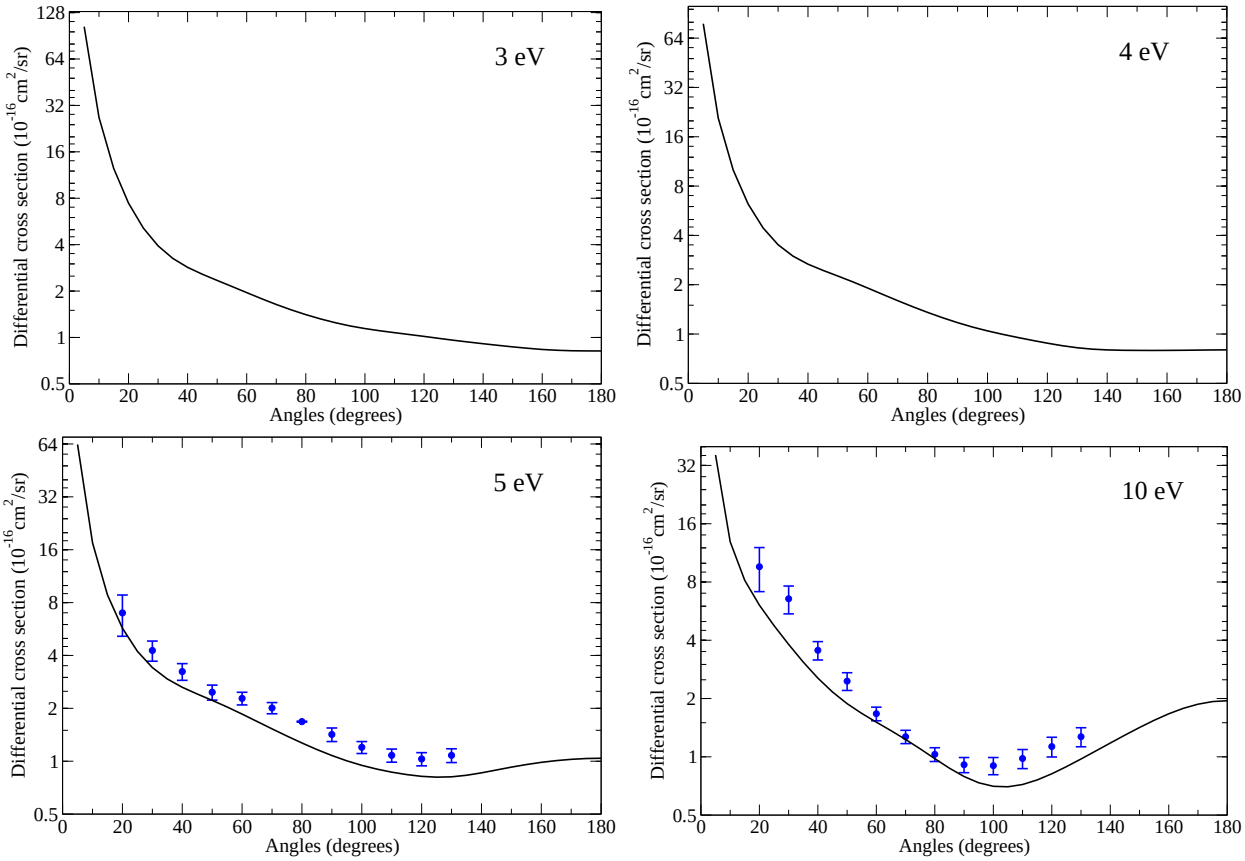


FIG. 3: (Color online) Electron scattering from formic acid: angular differential cross sections for different incident electron energies. Circles with error bars: experimental data of Vizcaino *et al.* [9]. Solid curve: complex Kohn calculations. Differential cross sections are in units of $10^{-16}$ cm$^2$/sr and energies are in eV.